Distribution of intracellular Ca^{2+}-ATPases in the mouse retina and their involvement in light-induced cone degeneration

David Martín-Oliva[#1], Sandra M. Martín-Guerrero[#1], M. Carmen Carrasco[1], Veronika E. Neubrand[1], María Martín-Estebané[1], José L. Marín-Teva[1], Julio Navascués[1], Miguel A. Cuadros[1], Peter Vangheluwe[2], M. Rosario Sepúlveda*[1]

[1] Department of Cell Biology, Faculty of Sciences, University of Granada, Granada, Spain

[2] Laboratory of Cellular Transport Systems, Department of Cellular and Molecular Medicine, KU Leuven, Leuven, Belgium

[#] These authors contributed equally to this work.

* **Corresponding author:** M. Rosario Sepúlveda. Department of Cell Biology, Faculty of Sciences, University of Granada. Avda. Fuentenueva s/n, 18071, Granada, Spain. Tel. +34 958 246334, mrsepulveda@ugr.es

Running title: SERCA2b and SPCA1 in mouse retina and cone photodegeneration

Highlights:

- Ca^{2+} pumps SERCA2b and SPCA1 are differentially distributed in adult mouse retina.
- SERCA2b and SPCA1 are highly expressed in cone photoreceptors.
- Light-induced stress in cone-661W cells affects SERCA2b and SPCA1 distribution.
- Organelle integrity can be recovered from light stress after washing and darkness.

ABSTRACT

Calcium signalling is involved in many processes in mammalian retina, from development to mature functions and neurodegeneration. Although proteins involved in Ca^{2+} entry in retinal cells have been well studied, less is known about Ca^{2+}-clearance. Among the Ca^{2+} pumps, plasma membrane Ca^{2+}-ATPases (PMCAs) have been identified as key proteins extruding Ca^{2+} across the plasma membrane with specific distribution in developing and adult retina. However, the two main isoforms of intracellular Ca^{2+}-ATPases in the central nervous system, the sarco(endo)plasmic reticulum (ER) Ca^{2+}-ATPase 2b (SERCA2b) and the secretory pathway Ca^{2+}-ATPase 1 (SPCA1), which remove cytosolic Ca^{2+} into intracellular stores, have been less or not at all analysed, respectively. In this study, we described for the first time the SPCA1 localisation in adult mouse retina and we report differential distributions of SERCA2b and SPCA1 transporters within various classes of retinal neurons and distinct subcellular localisations. In addition, we studied the expression and localisation of both Ca^{2+} pumps in 661W cells, a cone photoreceptor-derived cell line. Since continuous exposure to high light intensity induces photodegeneration, we analysed the effect of LED light exposure on these cells and SERCA2b and SPCA1 distribution. We found that continuous mild LED-light exposure compromised cell survival and produced stress in the ER and Golgi, the Ca^{2+} stores where the two pumps are localised. These effects were reversed after halting light exposure and washing. This study demonstrates that Ca^{2+} signalling may be involved in light-induced photoreceptor cell damage and points to previously unrecognised functions of intracellular Ca^{2+}-ATPases in retina physiology.

Keywords: SERCA2b, SPCA1, retina, cones, photoreceptors, 661W

Abbreviations: sarco(endo)endoplasmic reticulum Ca^{2+}-ATPase (SERCA), secretory pathway Ca^{2+}-ATPase (SPCA), plasma membrane Ca^{2+}-ATPase (PMCA), endoplasmic reticulum (ER), light emitting diode (LED).

1. INTRODUCTION

Excessive $[Ca^{2+}]_c$ has been related to retinal degenerative disorders [1], via over-activation of proteases such as calpain or caspases [2, 3] or increased stress in the endoplasmic reticulum (ER), the main intracellular Ca^{2+} store [4]. Many retinopathies such as macular degeneration are age-associated pathologies that cause blindness in the elderly [5]. Irrespective of age, people spend nowadays much more time in front of bright light emitted by the screen of electronic devices or are exposed to light emitting diode (LED) lights that are replacing conventional lights, which has been correlated with visual problems. Particularly, LED light emits large amounts of short wavelength and high-energy blue light that is harmful to cone photoreceptors [6, 7]. However, the underlying processes at the subcellular level, such as the Ca^{2+} signalling events that are involved in cellular damage of retinal cells, remain poorly studied.

The retina is a specialised tissue mainly formed by several layers of neurons interconnected by synapses. It converts incoming photons into action potentials that the visual cortex in the brain processes into three-dimensional images. Basically, six major neuronal cell types constitute the retina: Rods and cones photoreceptors are the light-sensitive cells, whose somata are located in the outer nuclear layer (ONL) of the retina and which form synapses with bipolar cells at the outer plexiform layer (OPL). Horizontal and amacrine neurons help to integrate and modulate this synaptic input. Both cell types, together with the bipolar cells, form the inner nuclear layer (INL). The bipolar cells contact the ganglion cells in the ganglion cell layer (GCL) and amacrine cells within the inner plexiform layer (IPL). Finally, the excitation of the ganglion cells, the sole output neurons of the retina, is transmitted via their axons, which constitute the optic nerve, and, thus propagate visual stimuli from the retina to the brain [8].

While Ca^{2+} entry-related proteins in retinal neurons have been studied in more detail [9-12] less is known about Ca^{2+} clearance mechanisms. Several Ca^{2+} transporters have been studied in the mammalian retina, mainly belonging to the plasma membrane Ca^{2+}-ATPase (PMCA) family. PMCA isoforms are key proteins extruding Ca^{2+} across the plasma membrane that present cell-type specific isoform distribution in adult and developing mammalian retina [13, 14]. In fact, alterations in the PMCA-mediated Ca^{2+} efflux have been related to photoreceptor cell death [15]. However, two other families of intracellular Ca^{2+}-ATPases that pump cytosolic Ca^{2+} to intracellular stores have been described in

mammalian cells: the sarco(endo)plasmic reticulum Ca^{2+}-transport ATPase (SERCA) and the secretory pathway Ca^{2+}-transport ATPase (SPCA). These transporters pump Ca^{2+} ions into the ER or into the trans-Golgi and vesicles of the secretory pathway, respectively (reviewed in [16, 17]). Whereas the presence of SERCA within the retina has been described earlier [18, 19], the expression and localisation of SPCA has not yet been studied in retinal cells.

In this work, we have analysed and compared the distribution of SERCA2b and SPCA1, the two most abundant isoforms of these transporters in the central nervous system, in the adult mouse retina. In particular, we focused on photoreceptors and performed *in vitro* experiments in the cone-derived 661W cell line to study the effect of light induced-photodegeneration on the cellular compartments where SERCA2b and SPCA1 pumps are localised.

2. MATERIAL AND METHODS

2.1 Animal and tissue preparation

Adult (3-months old) C57BL/6 mice or adult quails were obtained from the Animal Facility Service of the Scientific Instrumentation Centre from University of Granada. Animals were anaesthetized and perfused with 4% (w/v) paraformaldehyde in phosphate-buffered saline solution (PBS). All procedures were in accordance with the policies on the use of animals in research at the University of Granada. The eyeballs were isolated and postfixed by immersion in the same fixing solution for 24 h at 4°C. After rinse with PBS, tissue was cryo-protected in 10% (w/v) sucrose in PBS for 2 days, and then embedded in 10% (w/v) gelatine, 10% (w/v) sucrose in PBS. The blocks were frozen for 2 min in isopentane cooled at −60°C and stored at −80°C. Serial para-sagittal sections of 20 μm were obtained in a Leica CM1900 cryostat, collected on Super-Frost Plus slides, and conserved at −20ºC until use.

2.2 Immunohistochemistry

Cryostat sections were permeabilized by immersion in PBS-0.05% (v/v) Triton X-100 (PBS-T) for 15 min and blocked in a solution containing 0.2% (w/v) gelatin, 0.25% (v/v) Triton X-100 in PBS (PBS-G-T) and 0.1 M lysine for 1 h. Afterwards, sections were incubated overnight at room temperature in a humidified chamber with the polyclonal rabbit anti-SERCA2b antibody (1:500, [20]), the polyclonal rabbit anti-SPCA1 antibody (1:500, [21]), the lectin peanut agglutinin-FITC (1:500, Sigma-Aldrich, Cat No. L7381) or the monoclonal mouse cis-Golgi marker GM130 (1:500, BD Biosciences, Cat. No. 610822) diluted in PBS-G-T. Subsequently, sections were washed in PBS-T and incubated either with Alexa 594 goat anti-rabbit or with Alexa 488 goat anti-mouse secondary antibodies (Thermo Fisher Scientific, Cat. No. A11001 and A11012, respectively), both diluted 1:500 in PBS-G-T. Nuclei were stained with DAPI (10 μg/ml). Then, sections were covered with FluorSave medium (Calbiochem) and analysed using a Zeiss Axiophot fluorescence microscope with an Axiocam 506 color camera and the ZEN 2.3 Lite Software. Negative controls were performed for every set of experiments by omitting the primary antibodies from the procedure.

2.3 Cell culture

The murine photoreceptor-derived 661W cell line was a kind gift from Dr. Muayyad Al-Ubaidi (University of Oklahoma Health Sciences Center, Oklahoma City, OK). This cell line was previously characterised as a cone photoreceptor-cell linage [22]. Cells were maintained as adherent cultured monolayer in DMEM with 10% fetal bovine serum, L-glutamine 2 mM, streptomycin (100 µg/ml) and penicillin (100 U/ml), and incubated in a humidified atmosphere with 5% CO_2 at 37º C. Cells were seeded at a density of 2 x 10^6 cells per p100 plate, 10000 cells in 12 mm round-glass coverslips or 50000 cell per well in 96-well plates for Western blotting, immunocytochemistry and cell viability experiments, respectively.

2.4 Western Blotting

Mouse brain, mouse retina or 661W cells, previously washed in PBS and collected with a scraper, were used for membrane extract preparation following the protocol described in [23]. The protein content was evaluated by the Bio-Rad Protein Assay using bovine serum albumin (BSA) as protein standard. For Western blotting, 10 µg of membrane extracts were electrophoresed in 7.5% (w/v) SDS-polyacrylamide gels and transferred to polyvinylidene difluoride (PVDF) membranes using a Trans-Blot SD semidry system (Bio-Rad). After blocking in Tris-buffered saline (TBS) containing 5% (w/v) of non-fat dry milk and 0.3% Tween 20 for 1 h, immunological reactions were performed by incubating the PVDF membranes for 3 h at room temperature with the following primary antibodies diluted in TBS-1% (v/v) Tween 20: anti-SERCA2b (1:1000), anti-SPCA1 (1:1000), and the monoclonal mouse anti-β-actin (1:3000, Sigma-Aldrich, Cat. No. A5441) as loading control. Afterwards, PVDF membranes were incubated for 1 h at room temperature with peroxidase-conjugated goat anti-rabbit or goat anti-mouse secondary antibodies (1:5000, Sigma-Aldrich, Cat. No. A9169, A3682, respectively) and revealed with ECL substrate (Millipore) using a ChemiDoc-It (UVP) and VisionWorks LS software.

2.5 Immunocytochemistry in cultured cells

661W cells were fixed with 4% paraformaldehyde in PBS for 20 min, permeabilized with 0.2% (v/v) Triton X100 in PBS and blocked with 3% BSA in PBS for 1 h. Subcellular localisation of proteins were done by incubation with the anti-SERCA2b (1:500), the anti-SPCA1 (1:500), the anti-GM130 (1:500) or the monoclonal mouse anti-β tubulin primary antibodies (1:500, Sigma-Aldrich, Cat. No. T4026) diluted in the blocking solution for 1

h. Fluorescence labelling was obtained using secondary antibodies Alexa594 goat anti-rabbit and Alexa488 goat anti-mouse (1:2000) and DAPI for nuclei staining. Images were captured with the Zeiss Axiophot fluorescent microscope.

2.6 Photodegeneration assay

661W cells were seeded and incubated for 24 h in a humidified atmosphere of 5% CO_2 at 37ºC. The medium was replaced with media containing 1% FBS and returned to the incubator for 1 h before exposure to 1000 lux of light emitting diode-derived (LED) blue light for 24 h. The intensity of the emitted light was controlled by a luxometer HD9021 Delta Ohm SRL. Control cells were incubated in the same incubator in darkness by covering with aluminium foil. Cells stocks were not exposed to direct light at any time during passaging and feeding, nor were they maintained in any light–dark cycles.

2.7 Quantification of apoptotic cells

Cells were fixed and stained with DAPI for nuclear staining. Apoptotic cells were morphologically identified by their condensed chromatin and nucleus, which is smaller than the one of non-apoptotic cells.

2.8 MTT assay

Cell viability was determined by using 100 µg/ml 3-(4,5-dimethylthiazol-2-yl)-2,5-diphenyltetrazolium bromide (MTT) in PBS for 3 h at 37ºC in the incubator. Metabolically active cells reduced MTT to a formazan precipitate, which was solubilized in DMSO and quantified spectrophotometrically at 595 nm in a Multiskan Ascent microplate reader (Thermofisher). The percentage of viable cells was calculated considering that control cells in darkness were 100% viable.

2.9 Data processing and statistical analysis

Data were processed and analysed with the SigmaPlot v10 software (SPSS Inc, Chicago, IL) and presented as mean±S.E.M. Statistical comparisons were determined by unpaired Student´s t-test. Statistical significance was accepted when the p value was ≤ 0.05.

3. RESULTS

3.1 Expression and distribution of SERCA2b and SPCA1 in the adult retina

We analysed the distribution of intracellular Ca^{2+} pumps in cryostat sections of mouse retina by immunohistochemistry with the specific anti-SERCA2b and anti-SPCA1 antibodies. We observed a differential distribution of both pumps in retinal cell types and subcellular compartments (Fig. 1). SERCA2b was highly expressed in the outer segment of, presumably, cone photoreceptors. Weaker SERCA2b positive signals were also found in the myoid zone of inner segments and in the soma of all photoreceptors, located in the ONL. The SERCA2b antibody also labelled round cell bodies in the entire thickness of the INL and thin radial processes that emerge from these somata to the OPL and IPL, that morphologically resemble somata and axons of bipolar cells. On the other hand, SPCA1 showed strong immunoreaction in the inner segments of photoreceptors. In addition, a strong punctate staining appeared at the borders of the INL where the somata of horizontal and amacrine cells are localised, while a weak labelling appears in a few cells in the middle region. Ganglion cells expressed both intracellular Ca^{2+}-ATPases in the cell soma, although differences in the number of stained cells between both antibodies were found that could be due to the staining of different sets of retinal ganglion cells. Both plexiform layers were negative to immunostainings.

The anti-SERCA2b ER immunoreaction in the outer segment of cones was confirmed by staining with the peanut agglutinin lectin, a marker of cone photoreceptors that stains their plasma membrane [24] (Fig. 2A). We also performed double labelling with the Golgi marker GM130 and SPCA1 to determine its intracellular localisation (Fig. 2B). A colocalisation of both proteins in the Golgi apparatus of horizontal and amacrine cells was detected, although a small shift between both immunoreactions was observed representing cis- and trans-Golgi localisation, respectively.

Since the mouse is a nocturnal animal, with smaller number of cones than diurnal species, we also analysed the distribution of the intracellular Ca^{2+} pumps in the cone-enriched photoreceptor layer of the quail retina (Fig. 3). Both SERCA2b and SPCA1 showed similar staining as in the mouse, and, accordingly, SERCA2b was highly expressed in more outer segments in the quail retina.

3.2 Expression of SERCA2b and SPCA1 in 661W cells, a mouse cone photoreceptor-cell line

We turned to the murine cone photoreceptor-derived 661W cell line to further study the expression and subcellular localisation of the intracellular Ca^{2+} pumps SERCA2b and SPCA1. These cells show cellular and biochemical characteristics of cone photoreceptor cells [22]. First, we performed Western blot assays using protein extracts prepared from adult mouse retina, from 661W-cultured cells, and from adult mouse brain as a positive control with a high expression of SERCA2b and SPCA1 [25]. Results showed specific immunoreactions of SERCA2b (110 kDa) and SPCA1 (100 kDa) in the three analysed extracts (Fig. 4).

Via immunocytochemistry we analysed the subcellular distribution of both proteins in 661W cells using the same SERCA2b and SPCA1 antibodies in comparison to β-tubulin staining to visualise cell morphology (Fig. 5). We found SERCA2b spread from the perinuclear region throughout the cytoplasm in line with an ER localisation (Fig. 5A), whereas the SPCA1 pump was located in the juxtanuclear region at the Golgi apparatus, as confirmed by the Golgi marker GM130 (Fig. 5B).

3.3 Light-induced photodegeneration on 661W cells causes alterations in Ca^{2+} stores

Intense bright light exposure has been linked to retina pathologies and 661W cells are considered as a good *in vitro* model to study light-induced damage of photoreceptors [26, 27]. We here analysed if the Ca^{2+} stores of 661W cells containing the SERCA and SPCA Ca^{2+} transporters are affected by light-induced photodegeneration. We selected a mild light intensity with prolonged exposure to study early events in the subcellular compartments that can promote photoreceptor cell death. Additionally, we used reduced serum culture conditions that make cells much more susceptible to light stress [26]. Thus, 661W cells were exposed to 1000 lux of light-emitting diode (LED) for 24 h while control cells were kept in darkness. The LED light emission spectrum exhibited a main peak in the blue wavelengths (Fig. 6A). Blue LED light exposure induced changes in the 661W cellular morphology, with many cells rounded up and with apoptotic appearance (Fig. 6B). The number of apoptotic cells were significantly increased by light overexposure compared to controls (Fig. 6C). We also analysed the LED light effect on the subcellular distribution of SERCA2b and SPCA1 Ca^{2+} pumps. Cells exposed to LED light and immunostained with the SERCA2b antibody revealed two populations: cells showing normal integrity with some ER structural rearrangements, and other cells with a rounded morphology marked by condensed nuclear chromatin and a perinuclear aggregation of the SERCA2b-ER staining (Fig. 6D, E). Remarkably, the SPCA1 immunoreaction in

LED-exposed cells revealed the Golgi apparatus as a more susceptible Ca^{2+} store to light stress, since all cells with healthy nuclei lost the juxtanuclear Golgi-localisation, which appeared to be fragmented into smaller Golgi-derived stacks (Fig. 6D, E). Cells identified as apoptotic cells by their more condensed chromatin also showed condensed SPCA1-Golgi staining (Fig. 6E).

Since Golgi fragmentation is currently considered as an early symptom of neurodegeneration [28] that could be reversible at early stages [29], we here investigated the possibility of cell recovery from the photodegenerative insult (Fig. 7). Thus, after photodegeneration with 1000 lux of blue LED light for 24 h, cells were further incubated for additional 24 h in darkness. Alternatively, we also analysed the effect of replacement of the medium by fresh medium after the light exposure and a further incubation step for 24 h in darkness (Fig. 7A). Then, we determined cell viability of the cultures by MTT assays (Fig. 7B). While photodegeneration induced a reduction of cell viability to 61±2% compared to controls, a further 24 h of incubation in darkness did not rescue the cells. However, replacing the medium after the light insult and a further 24h-incubation in darkness halted the LED-induced cytotoxicity and allowed the culture to recover and even grow (117±9% after 24h recovery vs 61±2% after insult). Bright field images corroborated this recovery (Fig.7C). Immunocytochemistry with the anti-SERCA2b (Fig. 8A) and the anti-SPCA1 and anti-GM130 (Fig. 8B) antibodies after the recovery treatment also revealed a reestablishment of the organellar integrity of the intracellular Ca^{2+} stores where both Ca^{2+} pumps are located.

4. DISCUSSION

We report here for the first time the cellular and subcellular distribution of the SPCA1 Golgi Ca^{2+} pump in the adult mouse retina and we compare this with the ER Ca^{2+} pump SERCA2b. Both transporters were differentially distributed within various classes of retinal neurons and presented distinct subcellular localisations (Fig. 8), highlighting that functionally highly diverse populations of cells in the mouse retina most likely rely on different Ca^{2+} extrusion mechanisms. Besides SERCA and SPCA, the plasma membrane Ca^{2+} pump PMCA has been previously studied in retinal cells and presents a specific-isoform distribution in mouse retina [13], where photoreceptors selectively express PMCA1 and bipolar cells PMCA 1 and 2, while horizontal, amacrine and ganglion cells express PMCA2 and PMCA3. PMCA4 was highly expressed in plexiform layers consistent with its usual presence in synaptic terminals [30, 31]. Interestingly, SERCA2b and SPCA1 were not significantly detected in plexiform layers indicating their involvement in Ca^{2+} clearance in other subcellular areas that are not associated with synaptic transmission.

Noteworthy, the immunostaining patterns of SERCA2b we observed in mouse retina differed from earlier reports of amphibian [19], rat, squirrel [18] as well as mouse retina [18], presumably due to the use of general SERCA2 antibodies that recognize a and b splice variants in the earlier studies [18]. Several differences among species have been also reported with respect to the PMCA isoform localisation [13, 14, 19]. Overall, this suggests specific contributions to Ca^{2+} signalling among vertebrate visual systems.

Our findings that both SERCA2b and SPCA1 Ca^{2+} pumps label photoreceptors is not surprising since $[Ca^{2+}]_c$ plays a critical role in photoreceptor light adaptation [32] that even differs in rods and cones [33-35]. This is reflected by the differential expression of SERCA2b that we found in the outer segment of both photoreceptor types. Furthermore, Ca^{2+} signalling is atypical in photoreceptors, since $[Ca^{2+}]_c$ levels of resting cells in darkness is high [36], whereas light exposure induces a decrease of $[Ca^{2+}]_c$ that is proportional to the intensity of the background light [34]. The degree of lowered $[Ca^{2+}]_c$ depends on Ca^{2+} extrusion systems, which may involve the combined action of PMCA, SERCA and SPCA Ca^{2+} pumps. Thus, SERCA and SPCA in photoreceptors would transport Ca^{2+} into the ER and Golgi Ca^{2+} stores that can act either as sources or sinks of Ca^{2+}.

Interestingly, photoreceptors contain a continuous and dynamic ER cisternae network that extends from the inner segment to the perikaryon, which corresponds well with the SERCA2b localisation we observed. In fact, the highest Ca^{2+} concentration in photoreceptors is contained in the ER lumen [37], which suggests that the ER may represent the main site for dynamic control of cellular Ca^{2+} signal transductions. However, there is no a clear ER network in the outer segment of cones [38] where we also detected high SERCA2b expression, which appears controversial. Nevertheless, SERCA expression has been observed in the outer segments of cones in amphibia [19], and the inositol 1,4,5-triphosphate receptor, which releases Ca^{2+} from the ER store, has been detected in the outer segment of mammalian cones [39], supporting the presence of ER cisternae in that region.

In turn, the SPCA1 pump was present in Golgi cisternae of the inner segment of all photoreceptors, but also in the cell bodies of amacrine and horizontal cells, which are interneurons that modulate light-induced signals from photoreceptors. Although the Golgi apparatus does not store as much Ca^{2+} as the ER, a tight Ca^{2+} control within the Golgi is critical for neural polarity [40]. Photoreceptors are cells with a high and rapid turnover of phototransduction proteins, such as opsin and rhodopsin [41, 42]. This relies on the intracellular trafficking from the inner segment, the site of synthesis, to the outer segment, the site of phototransduction, and defects on this Golgi-dependent trafficking may lead to degeneration of photoreceptors.

Alterations or damage in the retina causes vision loss or even blindness. Increasing evidence shows that continuous exposure to short wavelength (blue) light leads to retinal cell damage [27]. Therefore, long-term exposure to light becomes a risk factor, especially in age-related macular degeneration, where cones are highly affected [43]. Apoptosis of photoreceptors in retinal degenerative disorders is well documented, but the molecular mechanisms are not well understood. It has been proposed that the photoreceptor cell death can be promoted by oxidative stress induced by reactive oxygen species (ROS), which was more increased by shorter than by longer wavelength light exposure [44]. In addition, ROS levels increase after LED light exposure in cone-derived 661W cells caused by the aggregation of S-opsin, which absorbs short wave-length light, as well as by ER stress [45]. The SERCA2b immunostaining in 661W cells also indicated signs of ER stress in our light-exposure experiments. Excessive ER stress leads to the release of Ca^{2+} from the ER lumen and induces mitochondrial Ca^{2+} accumulation, which, beyond a critical threshold, is one of the strongest inducers of the proapoptotic mitochondrial

membrane permeabilization, stimulating ROS production, release of cytochrome c and triggering cell death. Therefore, maintenance of ER Ca^{2+} homeostasis is vital in sustaining cellular functions during cellular stress [46], serving as a system to control pathologically high or low $[Ca^{2+}]_c$.

The LED-induced photodegeneration also disrupted the Golgi apparatus. Golgi fragmentation is found in many cell types, especially from the central nervous system, emerging as an early indicator of cell damage or death [28, 47], since Golgi fragmentation appears before strong ER stress and mitochondrial dysfunction. Although there are different types of Golgi fragmentation, they usually affect the main functions of the Golgi apparatus in protein secretion and modification as well as removal of excess Ca^{2+} from the cytoplasm. Thus, LED-induced Golgi fragmentation and segregation of the SPCA1 transporter in 661W cells may contribute to the effect on photodegeneration. Also, in a mouse deficient in the chaperone Hsp90α, which is related to retinitis pigmentosa, *i.e.* a disease leading to blindness, the Golgi apparatus is disrupted and impaired vesicle trafficking causes deformation of the outer segments of photoreceptors [48].

Golgi fragmentation appears as an early symptom of cell damage, which opens up strategies for recovery, since cell death programs have not yet been fully executed. We observed how the Golgi and ER integrity recovered after halting the exposure to 1000 lux-LED light for 24 h, a mild non-acute trigger. A similar recovery of Golgi integrity has been found in other cells after halting toxic treatments in early stages [29]. However, in the experiments described herein, the replacement of the culture medium with fresh medium was required for effective recovery, pointing out to a release of toxic molecules during the light exposure that contribute to photodegeneration.

In conclusion, our work highlights the intracellular Ca^{2+} transporters SPCA1 and SERCA2b in cell type-specific and spatially restricted systems for Ca^{2+} extrusion in the mouse retina. These Ca^{2+} pumps are responsible for Ca^{2+} sequestration into intracellular Ca^{2+} stores that may play a crucial role in the mechanisms underlying LED-light-induced cone damage, which is marked by ER stress and Golgi fragmentation and may compromise cell viability. A better understanding of the origin and reversibility of this organelle stress may open possibilities for therapies that halt photodegeneration.

ACKNOWLEDGEMENTS

We are very grateful to Prof C. Lillo (Dept. of Cell Biology and Pathology, University of Salamanca, Spain) for her gift of the peanut agglutinin-FITC and kind advice with retinal immunoreactions, and to Prof E. Hita (Dept. of Optics, University of Granada, Spain) for his help in LED-light spectrum determination. This work was supported by A1-CTS-324-UGR18 (MRS) from FEDER-Junta de Andalucia, Spain.

FIGURE LEGENDS

Figure 1 Localisation of SERCA2b and SPCA1 in the adult mouse retina. A. Immunofluorescence with anti-SERCA2b and anti-SPCA1 antibodies in mouse retina**.** Both proteins were expressed in photoreceptors. The SERCA2b (red, left panels) was highly expressed in outer segments (OS, short arrows), inner segments (IS, arrowheads) and somata (arrowheads in outer nuclear layer, ONL) of photoreceptors. SERCA2b was also found in the somata (arrowheads in inner nuclear layer, INL) and axons (large arrows) of cells in the INL corresponding to bipolar cells. The SPCA1 (red, right panels) was located in photoreceptor inner segments (arrowheads in IS) and in the somata of cells at the upper and lower border of the INL (arrowheads), where horizontal and amacrine cells are located. Ganglion cells expressed both intracellular Ca^{2+} pumps (asterisks), while plexiform layers were not immunolabelled. DAPI staining was used to visualise nuclei (blue) and to identify the nuclear layers of the retina. Scale bar: 20 µm. B. Schematic representation of the SERCA2b and SPCA1 localisation in the adult mouse retina. Neural cells are shaded in grey and SERCA2b and SPCA1 localisations are coloured in red and green, respectively. OPL, outer plexiform layer; IPL, inner plexiform layer; GCL, ganglion cell layer; r, rods; c, cones; hc, horizontal cells; bc, bipolar cells; ac, amacrine cell; gc, ganglion cells.

Figure 2 Localisation of SERCA2b in cone photoreceptors and of SPCA1 in horizontal and amacrine cells. A. Immunofluorescence with the anti-SERCA2b antibody (red) and co-staining with the cone photoreceptor marker peanut agglutinin lectin-FITC (green). Merged images showed the expression of SERCA2b staining in the cone outer segment. B. Double immunofluorescence of the anti-SPCA1 (red) antibody and the cis-Golgi marker GM130 (green) showing their colocalisation in the Golgi apparatus of horizontal cells (hc, short arrows) and amacrine cells (ac, arrowheads). DAPI staining was used to visualise the nuclei (blue). Regions in white boxes are shown in the insets with a higher magnification. OS/IS, outer segment and inner segment of photoreceptors; ONL, outer nuclear layer; INL, inner nuclear layer; IPL, inner plexiform layer. Scale bar: 10 µm.

Figure 3 Localisation of SERCA2b (A) and SPCA1 (B) in cone-enriched photoreceptor layer of the quail retina. SERCA2b was highly expressed in the outer

segment (arrows) of cone photoreceptors in the quail retina, that exhibited a high density of cones compared to mouse retina. Both SERCA2b and SPCA1 were also found in the inner segment of photoreceptors (arrowheads). DAPI staining was used to visualise nuclei. OS/IS, outer segment and inner segment of photoreceptors; ONL, outer nuclear layer. Scale bar: 20 µm.

Figure 4 Expression of SERCA2b and SPCA1 in mouse brain, mouse retina and in the mouse cone photoreceptor-derived 661W cells. Western blot assays showed specific immunoreactions of SERCA2b and SPCA1 in membrane extracts prepared from retina and 661W cells. Brain extracts were used as positive control for SERCA2b and SPCA1 expression, and β-actin as loading control.

Figure 5 Subcellular localisation of SERCA2b and SPCA1 in 661W cells. A. Double immunocytochemistry using the anti-SERCA2b antibody (red) to determine its subcellular localisation and the anti-β-tubulin antibody (green) to visualise cell morphology. SERCA2b was detected at the ER. B. Double immunofluorescence with the anti-SPCA1 (red) and the cis-Golgi marker GM130 (green) antibodies, showing Golgi localisation. DAPI staining (blue) was used to visualise nuclei. Scale bar: 10 µm.

Figure 6 Light-induced cell death in 661W cells. A. Spectrum of the LED light used in the photodegeneration experiments. A prominent peak around 450 nm corresponding to blue light is shown**.** B. Bright-field microscopy images of 661W cells exposed to 1000 lux of blue LED light for 24 h and control cells kept in darkness. Light-stressed cells showed a markedly round shape compared to control cells (magnifications are shown in insets). C. Quantification of apoptotic cells based on chromatin condensation in control and light-exposed cultures. Data are media ± SEM of four experiments in triplicates (*, $p \leq 0.05$). D. Immunoreactions with SERCA2b and SPCA1 antibodies in light-exposed 661W cells. LED light exposure induced a mild effect on the culture, with cells showing a strong condensated SERCA2b immunostaining into a round cell with apoptotic appearance after treatment (arrowheads) while other cells seemed to be less affected (arrows). However, a strong Golgi fragmentation (arrows) was observed by SPCA1 immunoreaction in LED-light overexposed cells compared to controls. E, F. Magnifications of LED-light overexposed cells stained with anti-SERCA2b (E) or anti-SPCA1 (F) antibodies (red) and DAPI to visualise nuclei (blue). Cells with healthy nuclei

showed structural rearrangements in the ER (E, arrow) and Golgi fragmentation (F, arrow), while apoptotic cells identified by condensed chromatin in the DAPI staining showed aggregation of the SERCA (E, arrowhead) and SPCA1 (F, arrowhead) immunostaining. Scale bars: B, 100 µm; D, 25 µm; F, 10 µm.

Figure 7 Cell recovery from the photodegenerative insult. A. The scheme represents experimental steps and incubation times to induce and halt LED light-induced photodegeneration. Cell media was replaced by 1% FBS-containing medium for 1 h and then cells were incubated in darkness (Ctr) or exposed to 1000 lux (LED light) for 24 h. In another condition, cells were further incubated for additional 24 h in darkness (Ctr + Darkness, and LED light + Darkness). Alternatively, cell medium was replaced by fresh medium after the insult and further incubated 24 h in darkness (Ctr + Wash + Darkness, and LED light + Wash + Darkness). B. Cell survival was scored by MTT assays after each experimental condition. Data are mean ± SEM (*, $p \leq 0.001$, comparing with Ctr; #, $p \leq 0.001$, comparing with LED light-exposed condition). C. Bright-field microscopy images of 661W cells in the four experimental conditions. Scale bar: 50 µm.

Figure 8 Integrity of Ca^{2+} stores can be recovered from the mild photodegenerative insult. A. Double immunofluorescence of anti-SERCA2b (red) and β-tubulin (green) after photodegeneration (LED light) or after cell recovery including washing with fresh medium and additional 24 h of incubation in darkness (LED light + recovery). Cells with condensed SERCA2b immunoreaction (arrowheads) were found only after LED light exposure. Surviving cells after the insult and after recovery exhibit an almost normal SERCA2b localisation with normal ER distribution throughout the cytoplasm (arrow). ~~E~~. B. Double immunofluorescence with anti-SPCA1 (red) and GM130 (green) in similar experiments as A. While all cells showed Golgi fragmentation (arrowheads) after the light exposure, almost all cells recovered the normal Golgi apparatus appearance and the SPCA1 immunoreaction (arrow). Nuclei were visualised by DAPI staining (blue). Scale bars: 25 µm.

REFERENCES

[1] S. Das, Y. Chen, J. Yan, G. Christensen, S. Belhadj, A. Tolone, F. Paquet-Durand, The role of cGMP-signalling and calcium-signalling in photoreceptor cell death: perspectives for therapy development, Pflugers Arch 473(9) (2021) 1411-1421.

[2] C.J. Zeiss, J. Neal, E.A. Johnson, Caspase-3 in postnatal retinal development and degeneration, Invest Ophthalmol Vis Sci 45(3) (2004) 964-70.

[3] J. Sancho-Pelluz, B. Arango-Gonzalez, S. Kustermann, F.J. Romero, T. van Veen, E. Zrenner, P. Ekstrom, F. Paquet-Durand, Photoreceptor cell death mechanisms in inherited retinal degeneration, Mol Neurobiol 38(3) (2008) 253-69.

[4] M.R. Butler, H. Ma, F. Yang, J. Belcher, Y.Z. Le, K. Mikoshiba, M. Biel, S. Michalakis, A. Iuso, D. Krizaj, X.Q. Ding, Endoplasmic reticulum (ER) Ca(2+)-channel activity contributes to ER stress and cone death in cyclic nucleotide-gated channel deficiency, J Biol Chem 292(27) (2017) 11189-11205.

[5] D. Bok, New insights and new approaches toward the study of age-related macular degeneration, Proc Natl Acad Sci U S A 99(23) (2002) 14619-21.

[6] C. Grimm, A. Wenzel, T. Williams, P. Rol, F. Hafezi, C. Reme, Rhodopsin-mediated blue-light damage to the rat retina: effect of photoreversal of bleaching, Invest Ophthalmol Vis Sci 42(2) (2001) 497-505.

[7] C. Roehlecke, U. Schumann, M. Ader, L. Knels, R.H. Funk, Influence of blue light on photoreceptors in a live retinal explant system, Mol Vis 17 (2011) 876-84.

[8] R.H. Masland, The neuronal organization of the retina, Neuron 76(2) (2012) 266-80.

[9] B. Williams, J.W. Maddox, A. Lee, Calcium Channels in Retinal Function and Disease, Annu Rev Vis Sci 8 (2022) 53-77.

[10] D. Krizaj, S. Cordeiro, O. Strauss, Retinal TRP channels: Cell-type-specific regulators of retinal homeostasis and multimodal integration, Prog Retin Eye Res 92 (2023) 101114.

[11] R. Rashwan, D.M. Hunt, L.S. Carvalho, The role of voltage-gated ion channels in visual function and disease in mammalian photoreceptors, Pflugers Arch 473(9) (2021) 1455-1468.

[12] M.J. Van Hook, S. Nawy, W.B. Thoreson, Voltage- and calcium-gated ion channels of neurons in the vertebrate retina, Prog Retin Eye Res 72 (2019) 100760.

[13] D. Krizaj, S.J. Demarco, J. Johnson, E.E. Strehler, D.R. Copenhagen, Cell-specific expression of plasma membrane calcium ATPase isoforms in retinal neurons, J Comp Neurol 451(1) (2002) 1-21.

[14] R.C. Renteria, E.E. Strehler, D.R. Copenhagen, D. Krizaj, Ontogeny of plasma membrane Ca2+ ATPase isoforms in the neural retina of the postnatal rat, Vis Neurosci 22(3) (2005) 263-74.

[15] A. Comitato, P. Subramanian, G. Turchiano, M. Montanari, S.P. Becerra, V. Marigo, Pigment epithelium-derived factor hinders photoreceptor cell death by reducing intracellular calcium in the degenerating retina, Cell Death Dis 9(5) (2018) 560.

[16] J. Chen, A. Sitsel, V. Benoy, M.R. Sepulveda, P. Vangheluwe, Primary Active Ca(2+) Transport Systems in Health and Disease, Cold Spring Harb Perspect Biol 12(2) (2020).

[17] P. Vangheluwe, M.R. Sepulveda, L. Missiaen, L. Raeymaekers, F. Wuytack, J. Vanoevelen, Intracellular Ca2+- and Mn2+-transport ATPases, Chem Rev 109(10) (2009) 4733-59.

[18] D. Krizaj, Serca isoform expression in the mammalian retina, Exp Eye Res 81(6) (2005) 690-9.

[19] D. Krizaj, X. Liu, D.R. Copenhagen, Expression of calcium transporters in the retina of the tiger salamander (Ambystoma tigrinum), J Comp Neurol 475(4) (2004) 463-80.

[20] F. Wuytack, J.A. Eggermont, L. Raeymaekers, L. Plessers, R. Casteels, Antibodies against the non-muscle isoform of the endoplasmic reticulum Ca2(+)-transport ATPase, Biochem J 264(3) (1989) 765-9.

[21] K. Van Baelen, J. Vanoevelen, G. Callewaert, J.B. Parys, H. De Smedt, L. Raeymaekers, R. Rizzuto, L. Missiaen, F. Wuytack, The contribution of the SPCA1 Ca2+ pump to the Ca2+ accumulation in the Golgi apparatus of HeLa cells assessed via RNA-mediated interference, Biochem Biophys Res Commun 306(2) (2003) 430-6.

[22] E. Tan, X.Q. Ding, A. Saadi, N. Agarwal, M.I. Naash, M.R. Al-Ubaidi, Expression of cone-photoreceptor-specific antigens in a cell line derived from retinal tumors in transgenic mice, Invest Ophthalmol Vis Sci 45(3) (2004) 764-8.

[23] J.M. Morales-Ropero, S. Arroyo-Urea, V.E. Neubrand, D. Martin-Oliva, J.L. Marin-Teva, M.A. Cuadros, P. Vangheluwe, J. Navascues, A.M. Mata, M.R. Sepulveda, The endoplasmic reticulum Ca(2+) -ATPase SERCA2b is upregulated in activated microglia and its inhibition causes opposite effects on migration and phagocytosis, Glia 69(4) (2021) 842-857.

[24] S. Herranz-Martin, D. Jimeno, A.E. Paniagua, A. Velasco, J.M. Lara, J. Aijon, C. Lillo, Immunocytochemical evidence of the localization of the Crumbs homologue 3 protein (CRB3) in the developing and mature mouse retina, PLoS One 7(11) (2012) e50511.

[25] M.R. Sepulveda, D. Marcos, M. Berrocal, L. Raeymaekers, A.M. Mata, F. Wuytack, Activity and localization of the secretory pathway Ca2+-ATPase isoform 1 (SPCA1) in different areas of the mouse brain during postnatal development, Mol Cell Neurosci 38(4) (2008) 461-73.

[26] Y. Kanan, G. Moiseyev, N. Agarwal, J.X. Ma, M.R. Al-Ubaidi, Light induces programmed cell death by activating multiple independent proteases in a cone photoreceptor cell line, Invest Ophthalmol Vis Sci 48(1) (2007) 40-51.

[27] Y. Kuse, K. Ogawa, K. Tsuruma, M. Shimazawa, H. Hara, Damage of photoreceptor-derived cells in culture induced by light emitting diode-derived blue light, Sci Rep 4 (2014) 5223.

[28] N.K. Gonatas, A. Stieber, J.O. Gonatas, Fragmentation of the Golgi apparatus in neurodegenerative diseases and cell death, J Neurol Sci 246(1-2) (2006) 21-30.

[29] M.R. Sepulveda, F. Wuytack, A.M. Mata, High levels of Mn(2)(+) inhibit secretory pathway Ca(2)(+)/Mn(2)(+)-ATPase (SPCA) activity and cause Golgi fragmentation in neurons and glia, J Neurochem 123(5) (2012) 824-36.

[30] M.R. Sepulveda, M. Berrocal-Carrillo, M. Gasset, A.M. Mata, The plasma membrane Ca2+-ATPase isoform 4 is localized in lipid rafts of cerebellum synaptic plasma membranes, J Biol Chem 281(1) (2006) 447-53.

[31] R. Padanyi, K. Paszty, E.E. Strehler, A. Enyedi, PSD-95 mediates membrane clustering of the human plasma membrane Ca2+ pump isoform 4b, Biochim Biophys Acta 1793(6) (2009) 1023-32.

[32] H.R. Matthews, R.L. Murphy, G.L. Fain, T.D. Lamb, Photoreceptor light adaptation is mediated by cytoplasmic calcium concentration, Nature 334(6177) (1988) 67-9.

[33] K. Nakatani, K.W. Yau, Calcium and light adaptation in retinal rods and cones, Nature 334(6177) (1988) 69-71.

[34] A.P. Sampath, H.R. Matthews, M.C. Cornwall, J. Bandarchi, G.L. Fain, Light-dependent changes in outer segment free-Ca2+ concentration in salamander cone photoreceptors, J Gen Physiol 113(2) (1999) 267-77.

[35] R.J. Perry, P.A. McNaughton, Response properties of cones from the retina of the tiger salamander, J Physiol 433 (1991) 561-87.

[36] M.L. Woodruff, A.P. Sampath, H.R. Matthews, N.V. Krasnoperova, J. Lem, G.L. Fain, Measurement of cytoplasmic calcium concentration in the rods of wild-type and transducin knock-out mice, J Physiol 542(Pt 3) (2002) 843-54.

[37] F. Ungar, I. Piscopo, E. Holtzman, Calcium accumulation in intracellular compartments of frog retinal rod photoreceptors, Brain Res 205(1) (1981) 200-6.

[38] A.M. Mercurio, E. Holtzman, Smooth endoplasmic reticulum and other agranular reticulum in frog retinal photoreceptors, J Neurocytol 11(2) (1982) 263-93.

[39] T.L. Wang, P. Sterling, N. Vardi, Localization of type I inositol 1,4,5-triphosphate receptor in the outer segments of mammalian cones, J Neurosci 19(11) (1999) 4221-8.

[40] M.R. Sepulveda, J. Vanoevelen, L. Raeymaekers, A.M. Mata, F. Wuytack, Silencing the SPCA1 (secretory pathway Ca2+-ATPase isoform 1) impairs Ca2+ homeostasis in the Golgi and disturbs neural polarity, J Neurosci 29(39) (2009) 12174-82.

[41] D. Deretic, Post-Golgi trafficking of rhodopsin in retinal photoreceptors, Eye (Lond) 12 (Pt 3b) (1998) 526-30.

[42] R. Schmied, E. Holtzman, Involvement of the Golgi apparatus in sorting of materials to opposite ends of frog rod retinal photoreceptors, J Neurobiol 20(3) (1989) 115-38.

[43] J.M. Seddon, C.A. Chen, The epidemiology of age-related macular degeneration, Int Ophthalmol Clin 44(4) (2004) 17-39.

[44] M. Rozanowska, J. Wessels, M. Boulton, J.M. Burke, M.A. Rodgers, T.G. Truscott, T. Sarna, Blue light-induced singlet oxygen generation by retinal lipofuscin in non-polar media, Free Radic Biol Med 24(7-8) (1998) 1107-12.

[45] T. Nakanishi, M. Shimazawa, S. Sugitani, T. Kudo, S. Imai, Y. Inokuchi, K. Tsuruma, H. Hara, Role of endoplasmic reticulum stress in light-induced photoreceptor degeneration in mice, J Neurochem 125(1) (2013) 111-24.

[46] J. Groenendyk, L.B. Agellon, M. Michalak, Calcium signaling and endoplasmic reticulum stress, Int Rev Cell Mol Biol 363 (2021) 1-20.

[47] C. Makhoul, P. Gosavi, P.A. Gleeson, Golgi Dynamics: The Morphology of the Mammalian Golgi Apparatus in Health and Disease, Front Cell Dev Biol 7 (2019) 112.

[48] Y. Wu, X. Zheng, Y. Ding, M. Zhou, Z. Wei, T. Liu, K. Liao, The molecular chaperone Hsp90alpha deficiency causes retinal degeneration by disrupting Golgi organization and vesicle transportation in photoreceptors, J Mol Cell Biol 12(3) (2020) 216-229.

FIGURE 1

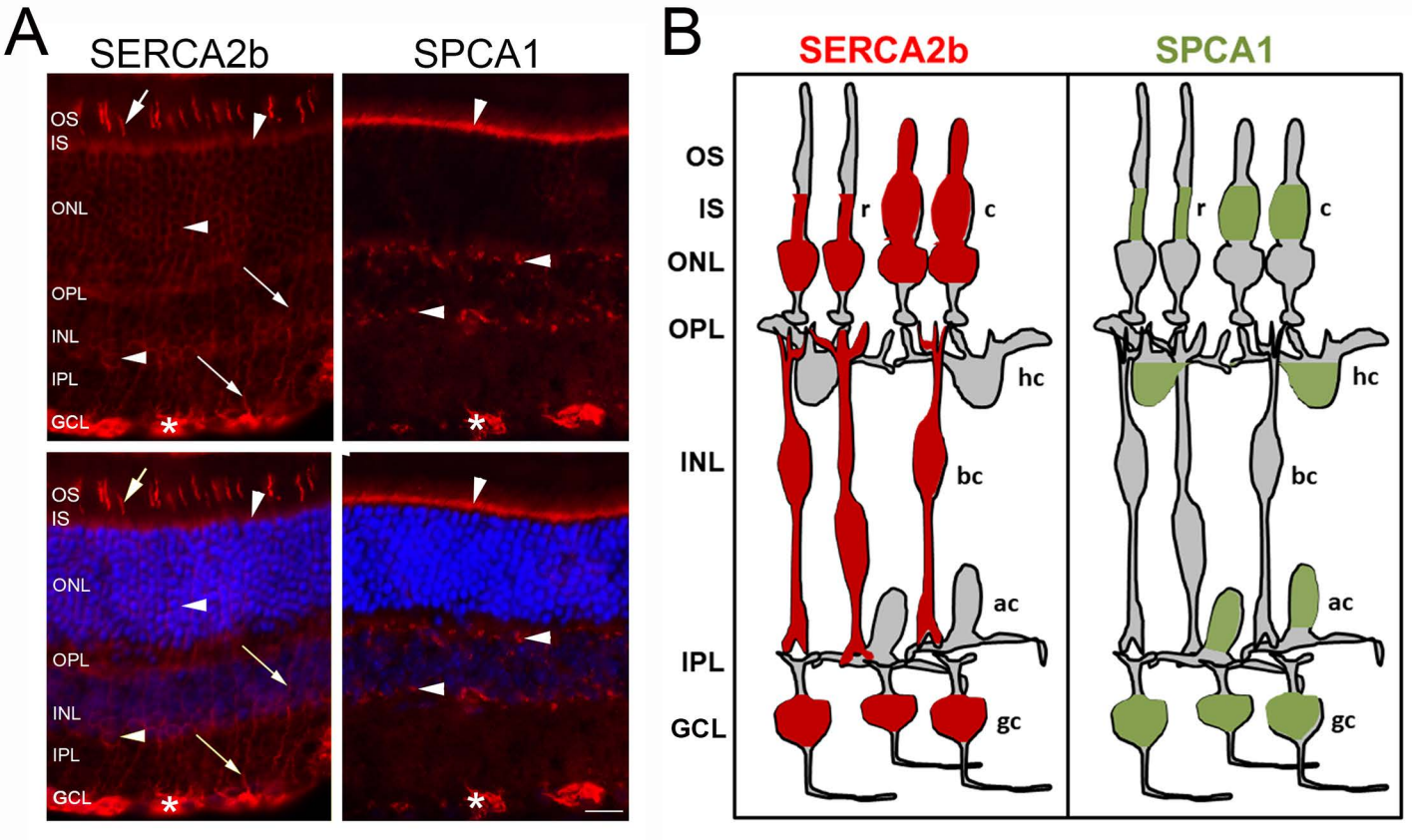
A
SERCA2b
SPCA1
OS
IS
ONL
OPL
INL
IPL
GCL
B
SERCA2b
SPCA1
OS
IS
ONL
OPL
INL
IPL
GCL
r
c
hc
bc
ac
gc

FIGURE 2

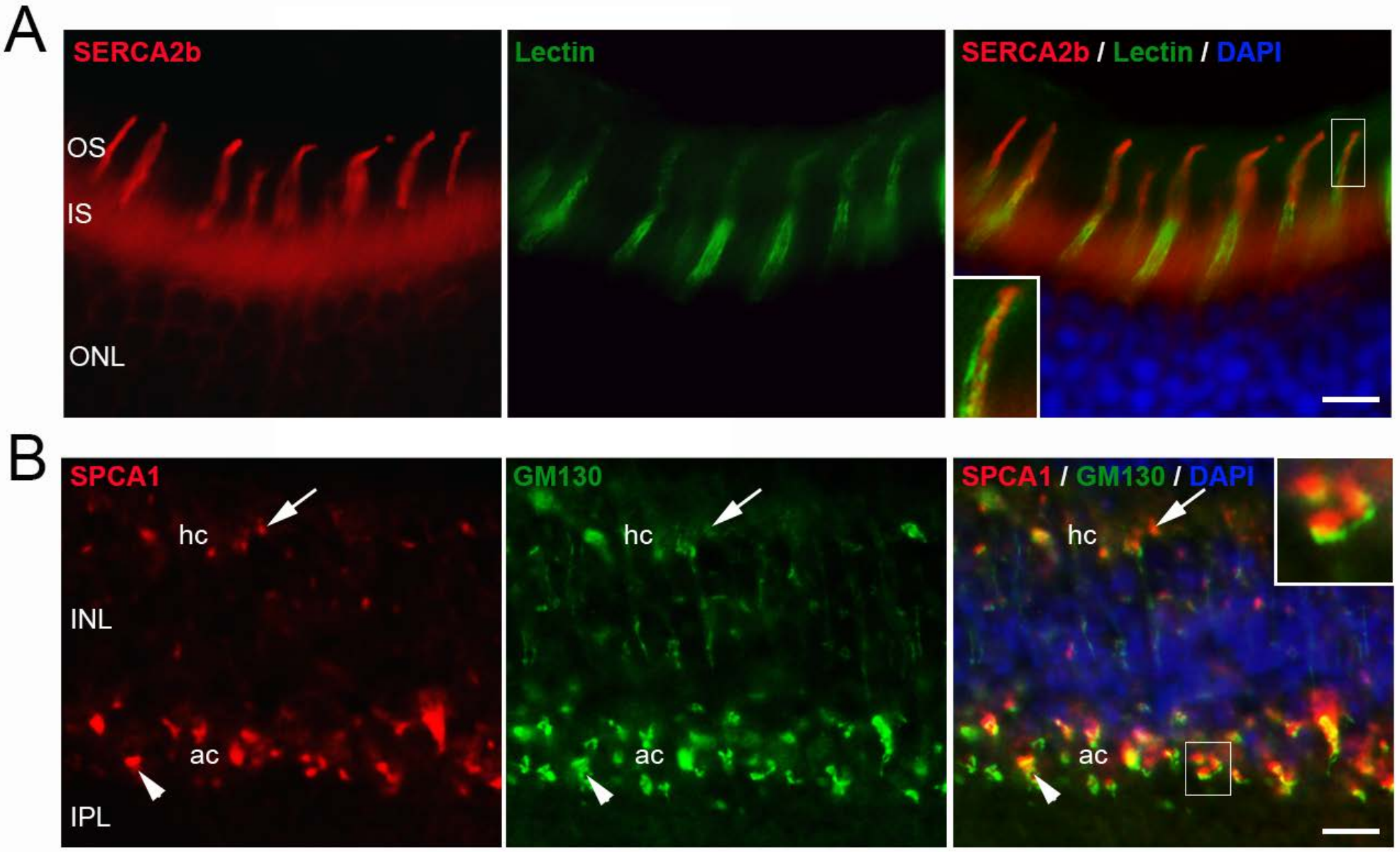
A
SERCA2b
OS
IS
ONL
Lectin
SERCA2b / Lectin / DAPI
B
SPCA1
hc
INL
ac
IPL
GM130
hc
ac
SPCA1 / GM130 / DAPI
hc
ac

FIGURE 3

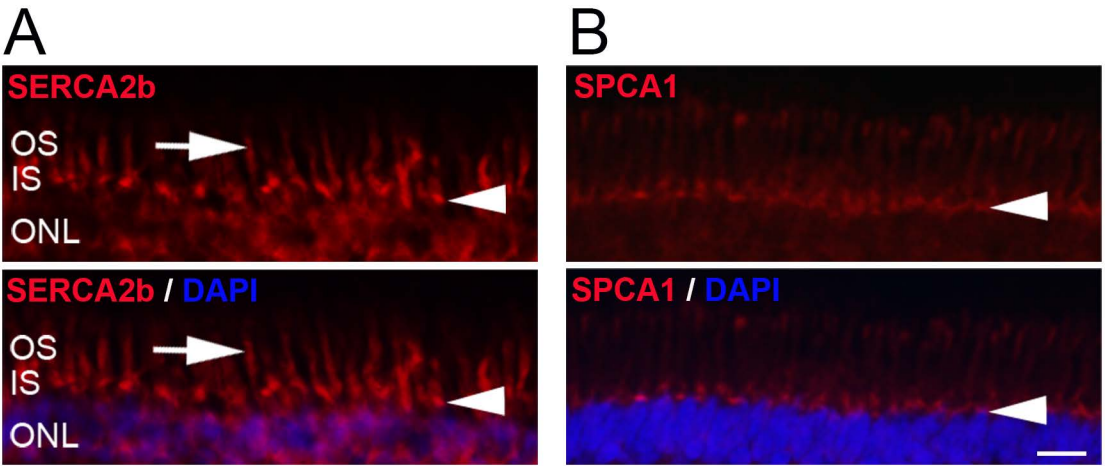
A
SERCA2b
OS
IS
ONL
SERCA2b / DAPI
OS
IS
ONL
B
SPCA1
SPCA1 / DAPI

FIGURE 4

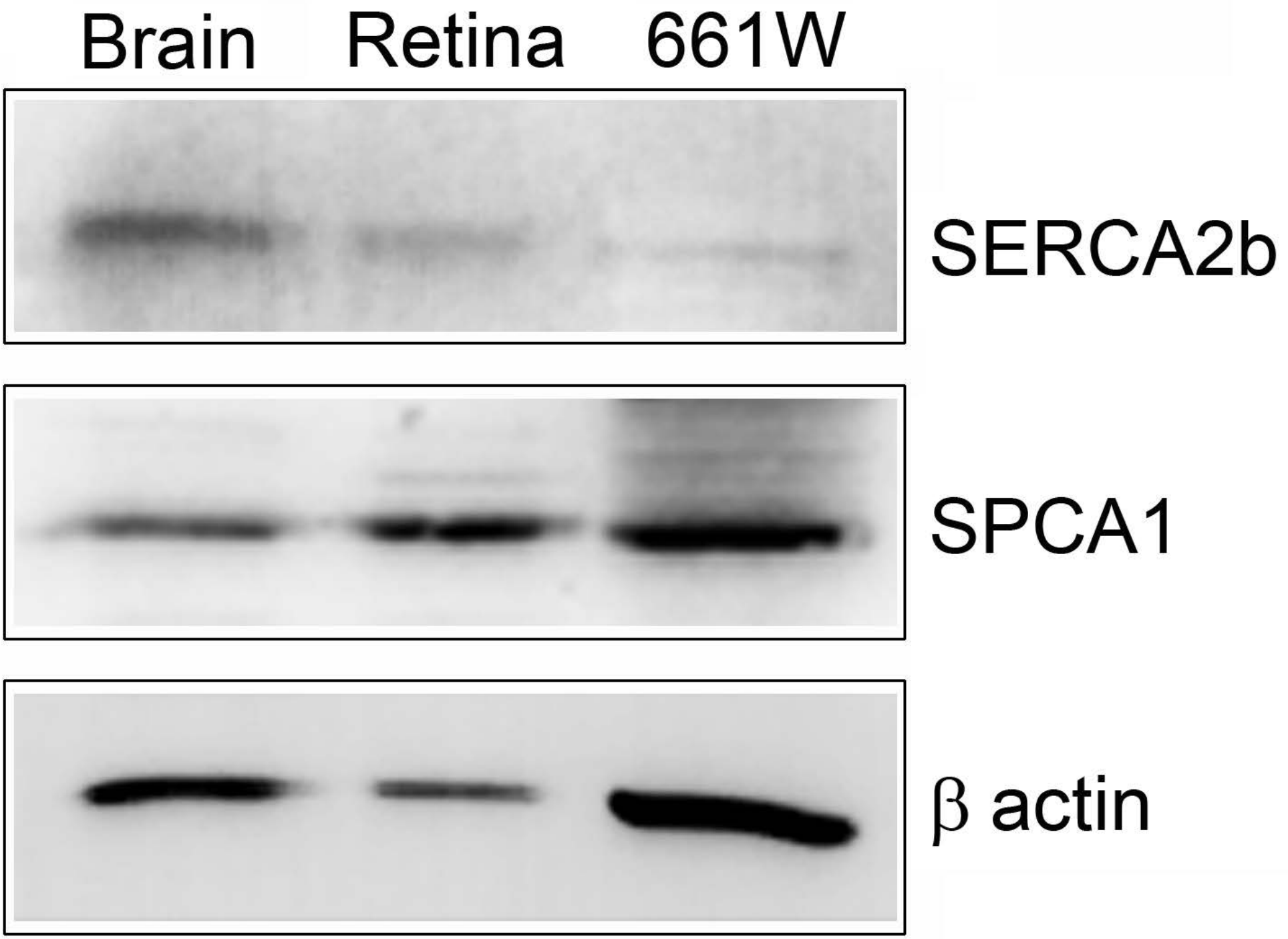
Brain
Retina
661W
SERCA2b
SPCA1
β actin

FIGURE 5

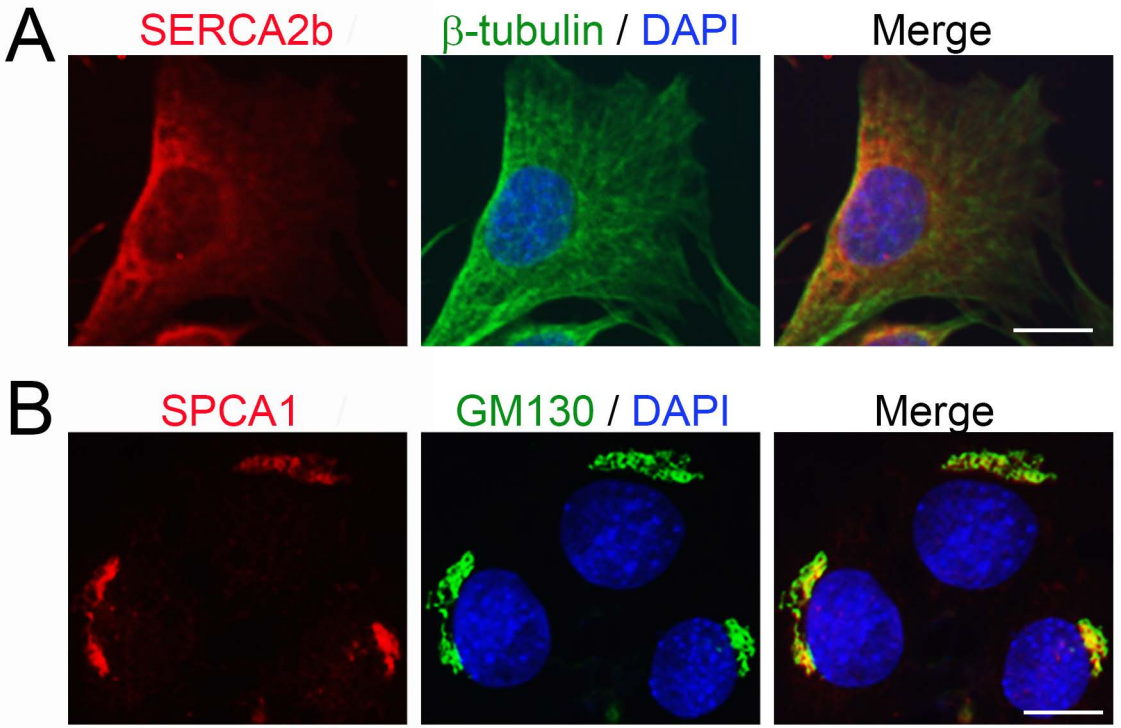
A
SERCA2b
β-tubulin / DAPI
Merge
B
SPCA1
GM130 / DAPI
Merge

FIGURE 6

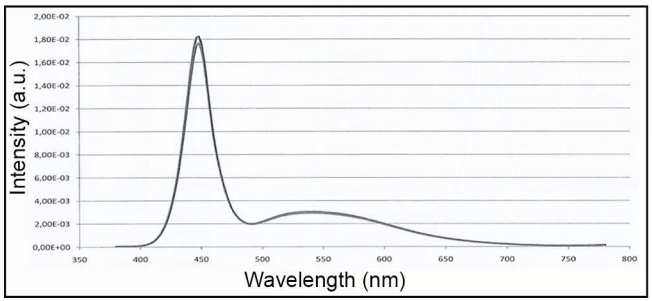
A
Intensity (a.u.)
Wavelength (nm)

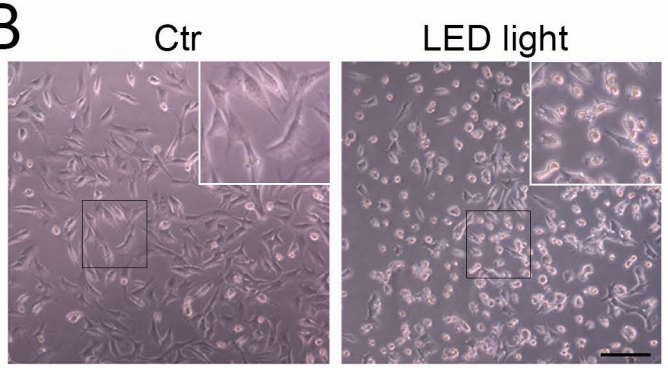
B
Ctr
LED light

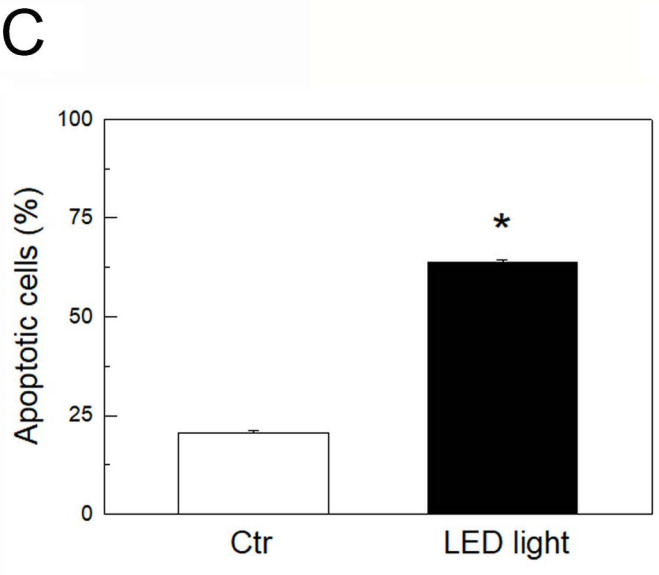
C
Apoptotic cells (%)
100
75
50
25
0
*
Ctr
LED light

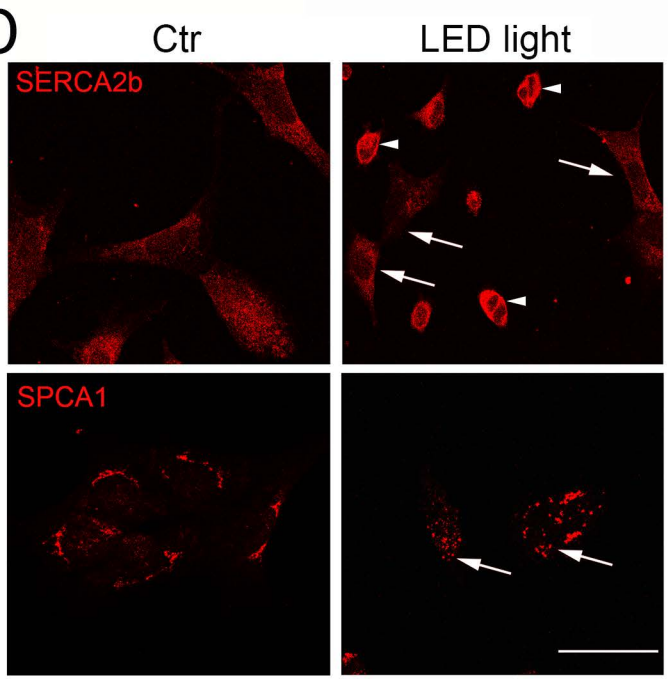
D
Ctr
LED light
SERCA2b
SPCA1

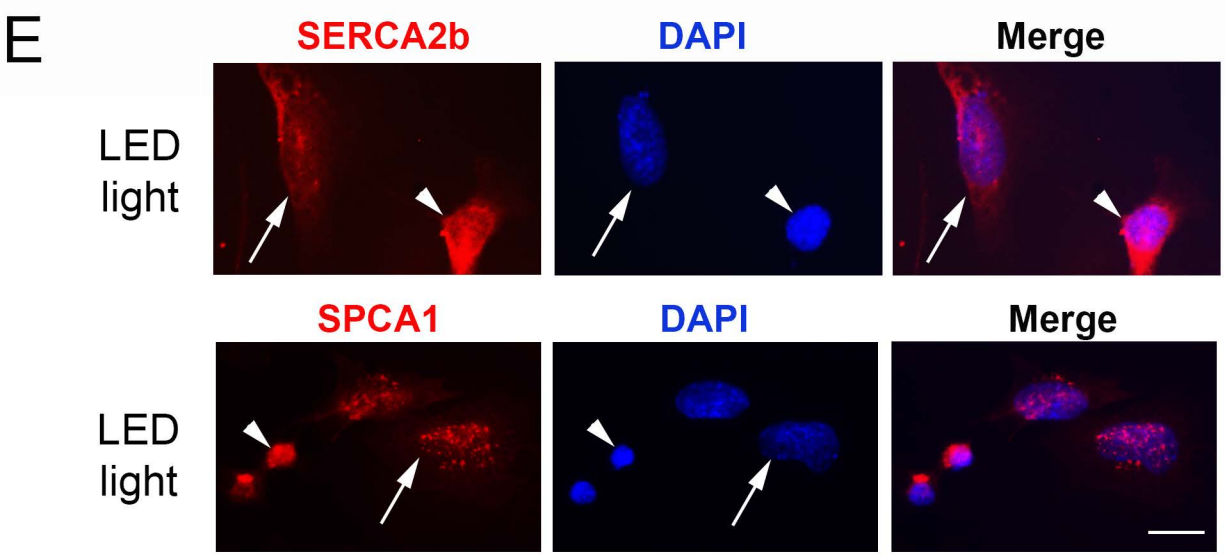
E
SERCA2b
DAPI
Merge
LED light
SPCA1
DAPI
Merge
LED light

FIGURE 7

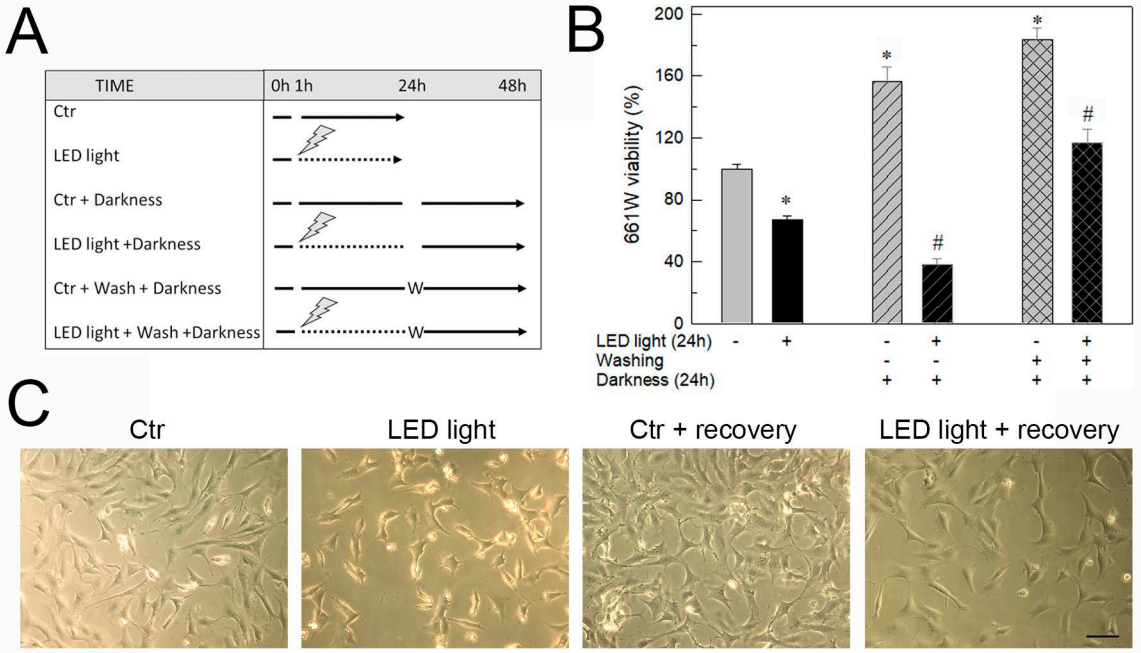
A
TIME
0h 1h
24h
48h
Ctr
LED light
Ctr + Darkness
LED light +Darkness
Ctr + Wash + Darkness
W
LED light + Wash +Darkness
W
B
661W viability (%)
200
160
120
80
40
0
*
*
*
#
#
LED light (24h) - + - + - +
Washing - - + + + +
Darkness (24h) + + + + + +
C
Ctr
LED light
Ctr + recovery
LED light + recovery

FIGURE 8

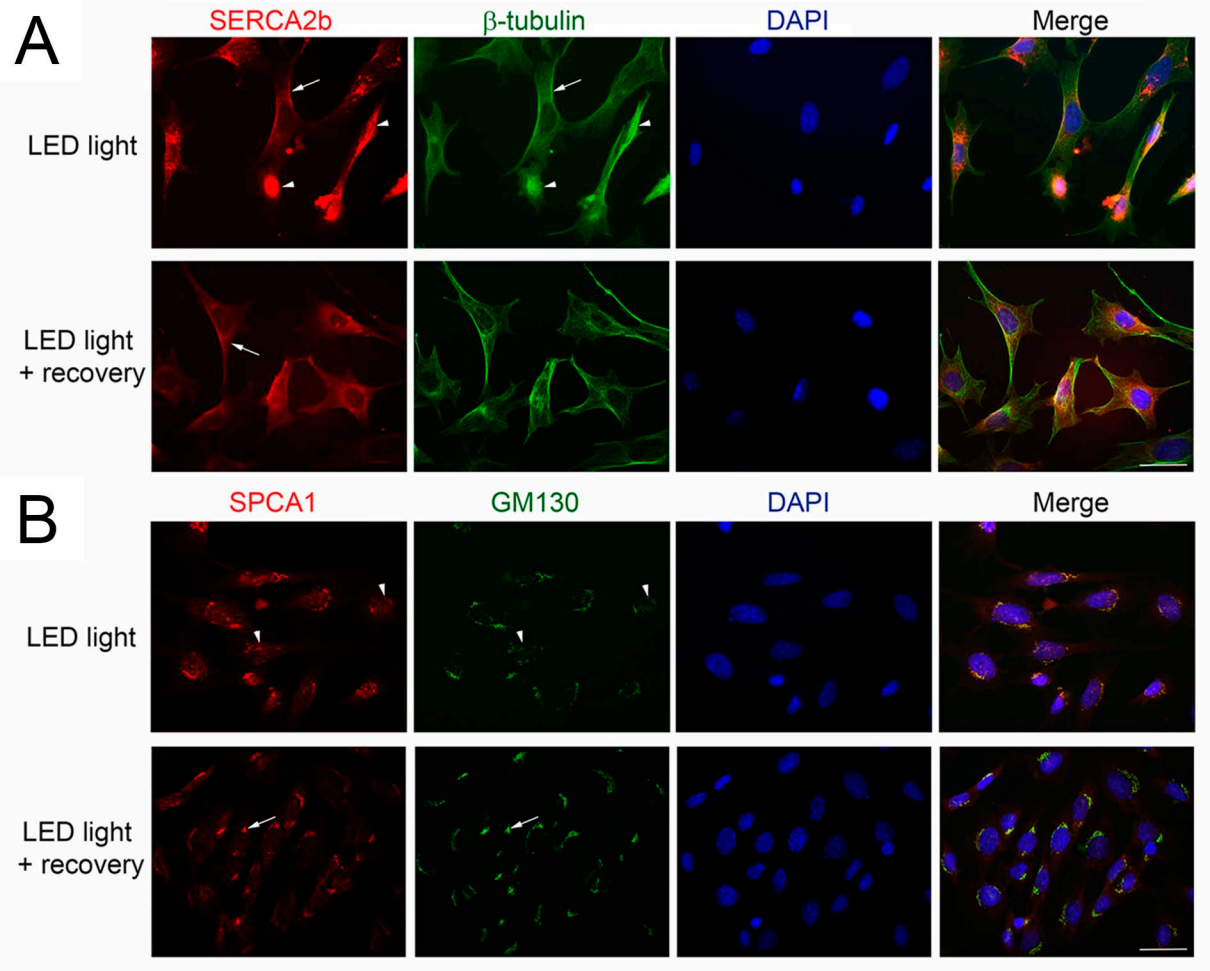
A
SERCA2b
β-tubulin
DAPI
Merge
LED light
LED light
+ recovery
B
SPCA1
GM130
DAPI
Merge
LED light
LED light
+ recovery